

## Identification of Diet-Derived Constituents as Potent Inhibitors of Intestinal Glucuronidation

Brandon T. Gufford, Gang Chen, Philip Lazarus, Tyler N. Graf, Nicholas H. Oberlies, and Mary F. Paine

Section of Experimental and Systems Pharmacology (B.T.G., M.F.P.) and Department of Pharmaceutical Sciences (G.C., P.L.), College of Pharmacy, Washington State University, Spokane, Washington; and Department of Chemistry and Biochemistry, University of North Carolina at Greensboro, Greensboro, North Carolina (T.N.G., N.H.O.)

Running Title: Diet-Derived Inhibitors of Intestinal Glucuronidation

Corresponding Author: Mary F. Paine, RPh, PhD  
Experimental and Systems Pharmacology  
WSU College of Pharmacy  
PBS 323, PO Box 1495  
Spokane, WA 99210-1495  
Phone: 509-358-7759  
Fax: 509-368-6561  
Email: mary.paine@wsu.edu

Number of text pages: 18

Number of tables: 2

Number of figures: 6

Number of references: 56

Word Count

Total: 4,511

Abstract: 231

Introduction: 695

Discussion: 1,453

Abbreviations: BSA, bovine serum albumin; CYP, cytochrome P450; EGCG, epigallocatechin gallate; HEK, human embryonic kidney; HIM, human intestinal microsome; HLM, human liver microsome; 4-MU, 4-methylumbelliferone; MPA, mycophenolic acid; UDPGA, UDP-glucuronic acid; UGT, UDP-glucuronosyl transferase; UHPLC, ultra high-performance liquid chromatography

## Abstract

Drug metabolizing enzymes within enterocytes constitute a key barrier to xenobiotic entry into the systemic circulation. Furanocoumarins in grapefruit juice are cornerstone examples of diet-derived xenobiotics that perpetrate interactions with drugs via mechanism-based inhibition of intestinal cytochrome P450 3A4 (CYP3A4). Relative to intestinal CYP3A4-mediated inhibition, alternate mechanisms underlying dietary substance-drug interactions remain understudied. A working systematic approach was applied to a panel of structurally diverse diet-derived constituents/extracts (n=15) as inhibitors of intestinal UDP-glucuronosyl transferases (UGTs) to identify and characterize additional perpetrators of dietary substance-drug interactions. Using a screening assay involving the non-specific UGT probe substrate 4-methylumbelliferone, human intestinal microsomes, and human embryonic kidney cell lysates overexpressing gut-relevant UGT1A isoforms, 14 diet-derived constituents/extracts inhibited UGT activity by >50% in at least one enzyme source, prompting IC<sub>50</sub> determination. The IC<sub>50</sub> of 13 constituents/extracts (≤10 μM with at least one enzyme source) was well below intestinal tissue concentrations or concentrations in relevant juices, suggesting that these diet-derived substances can inhibit intestinal UGTs at clinically achievable concentrations. Evaluation of inhibitor depletion on IC<sub>50</sub> determination demonstrated substantial impact (up to 2.8-fold shift) using silybin A and silybin B, two key flavonolignans from milk thistle (*Silybum marianum*) as exemplar inhibitors, highlighting an important consideration for interpretation of UGT inhibition in vitro. Results from this work will help refine a working systematic framework to identify dietary substance-drug interactions that warrant advanced modeling and simulation to inform clinical assessment.

## Introduction

The gastrointestinal tract represents the first portal to xenobiotics taken orally, including myriad drugs and diet-derived substances. Consequently, such xenobiotics must traverse the intestinal epithelial barrier before entering the hepatic venous, and eventually systemic, circulation. This barrier is composed primarily of enterocytes that, like hepatocytes, express a plethora of biotransformation enzymes that can influence significantly the extent of presystemic (first-pass) xenobiotic metabolism (Won et al., 2012). Accordingly, inhibition of intestinal enzymes can lead to an increase in hepatic and systemic exposure to the 'victim' xenobiotic with the subsequent potential for unwanted effects. A well-studied 'perpetrator' diet-derived substance is grapefruit juice, which contains furanocoumarins that inhibit intestinal cytochrome P450 (CYP) 3A4 via mechanism-based inhibition with subsequent protein degradation (Paine and Oberlies, 2007). More than 85 medications are vulnerable to the 'grapefruit juice effect', of which the labeling for several includes cautionary statements (Bailey et al., 2013).

Relative to intestinal CYP3A4-mediated inhibition, alternate mechanisms underlying dietary substance-drug interactions remain understudied. Many drugs and diet-derived constituents, particularly polyphenolic molecules, undergo extensive pre-systemic phase II metabolism in both the gut and the liver, with glucuronidation typically predominating in humans (Ritter, 2007; Wu et al., 2011). Drug molecules seldom inhibit this process with sufficient potency to overcome the low affinity and high capacity of the UDP-glucuronosyl transferases (UGTs). Accordingly, drugs rarely perpetrate clinically relevant UGT-mediated interactions (Williams et al., 2004). In contrast, diet-derived constituents have shown greater inhibitory potency towards UGT activity than most drugs, including those considered prototypic UGT inhibitors, such as some nonsteroidal anti-inflammatory agents, benzodiazepines, and immunosuppressants (Kiang et al., 2005; Mohamed et al., 2010; Mohamed and Frye, 2011a; Mohamed and Frye, 2011b; Li et al., 2012).

Diet-derived constituent concentrations in enterocytes typically are much higher than systemic concentrations, especially when considering unconjugated constituents. This contention was demonstrated following oral administration of the semi-purified milk thistle (*Silybum marianum*) extract, silibinin (1400 mg), of which mean colorectal tissue concentrations were more than 50-fold higher than systemic concentrations (~140 versus 2.5  $\mu\text{M}$ ) (Hoh et al., 2006). High enteric concentrations, coupled with the high inhibitory potencies of diet-derived constituents/extracts towards enteric glucuronidation, raise concern for clinically relevant dietary substance-drug interactions mediated via inhibition of intestinal UGTs.

Despite growing recognition of the potential for dietary substance-drug interactions, systematic approaches to identify and characterize the risk of these interactions remain elusive (Won et al., 2012; Brantley et al., 2014a). Considerations unique to evaluation of UGT inhibition, including luminal orientation of UGT proteins requiring detergents or pore-forming agents to reduce latency, limited availability of authentic glucuronide standards, and a lack of isoform selective probe substrates and inhibitors, have further hampered efforts to correlate in vitro inhibitory potency with in vivo interaction risk. Rapid clearance of UGT substrates, as well as inhibitors, likely violates assumptions applicable to inhibitory assay conditions developed using enzyme systems with lower metabolic capacity and higher affinity such as CYPs (i.e., minimal substrate and inhibitor depletion). As such, traditional approaches used to evaluate drug interaction liability may not be applicable to UGT-mediated interactions. In addition to experimental considerations, the highly variable composition and structural diversity of dietary substances further complicates evaluation of drug interaction liability. Interaction risk is compounded by the relative lack of regulatory oversight to guide dosing recommendations, safety assessment, and chronic use of dietary substances. As proposed, examination of isolated constituents would facilitate development of systematic approaches (Brantley et al., 2013). A systematic evaluation of isolated dietary substance constituents as inhibitors of intestinal UGTs, including gut-specific isoforms, has not been reported.

The objective of this study was to evaluate selected diet-derived constituents/extracts as inhibitors of intestinal glucuronidation. The aims were to (1) test a panel of dietary constituents and extracts using the non-specific UGT probe substrate 4-methylumbelliferone (4-MU), human intestinal microsomes (HIMs), and UGT1A-overexpressing human embryonic kidney (HEK293) cell lysates; (2) determine the inhibition potency ( $IC_{50}$ ) of selected constituents/extracts; and (3) prioritize constituents/extracts for further evaluation. Results will help refine a working systematic framework for identification of dietary substance-drug interactions that warrant advanced modeling and simulation to inform clinical assessment. Ultimately, these efforts will help to provide evidence-based recommendations to both clinicians and consumers about the safety or risk of taking certain dietary substances with conventional medications.

## **Materials and Methods**

### **Materials and Chemicals**

Human liver (pooled from 50 donors, mixed gender) and intestinal (pooled from 13 donors, mixed gender) microsomes (HLMs and HIMs, respectively) were purchased from Xenotech, LLC (Lenexa, KS). HEK293 cells over-expressing individual UGT1A enzymes were harvested and homogenates prepared as described previously (Sun et al., 2013). Alamethicin, bovine serum albumin (BSA), diclofenac, epigallocatechin gallate (EGCG), magnesium chloride, 4-MU, naringin, nicardipine, saccharolactone, silibinin, and UDP-glucuronic acid (UDPGA) were purchased from Sigma-Aldrich (St. Louis, MO). Apigenin, kaempferol, naringenin, and quercetin were purchased from Cayman Chemical Company (Ann Arbor, MI). Silymarin was obtained from Euromed S.A. (Barcelona, Spain) and consisted of the flavonolignans silybin A (16%), silybin B (24%), isosilybin A (6.4%), isosilybin B (4.4%), silydianin (17%), silychristin (12%), and isosilychristin (2.2%); the remainder consisted of the flavonoid taxifolin (1.6%) and uncharacterized polyphenols and aliphatic fatty acids (Davis-Searles et al., 2005). The individual flavonolignans were purified as described previously (Graf et al., 2007) and were >97% pure as determined by UHPLC (Napolitano et al., 2013). Methanol (LC/MS grade), ethanol, Tris-HCl, Tris base, and formic acid were purchased from Fisher Scientific (Waltham, MA).

### **Evaluation of Milk Thistle Flavonolignans and other Diet-Derived Constituents as Inhibitors of Intestinal UGT Activity**

Milk thistle flavonolignans (silybin A, silybin B, isosilybin A, isosilybin B, silychristin, isosilychristin, silydianin) and associated extracts (silibinin, silymarin) and other, structurally diverse diet-derived constituents (naringin, naringenin, apigenin, kaempferol, quercetin, EGCG) (Supplemental Fig. 1) were evaluated as inhibitors of intestinal UGT activity using 4-MU, HIMs, and HEK293 cell lysates overexpressing the gut-relevant UGT isoforms UGT1A1, UGT1A8, and UGT1A10. Inhibition of hepatic glucuronidation by HLMs was evaluated as a comparator for the intestinal systems, as well as literature values obtained from hepatic systems. 4-MU, diclofenac,

nicardipine, and each dietary constituent/extract were dissolved in methanol to yield 40 mM stock solutions. UDPGA was prepared fresh in Tris-HCl buffer (100 mM, pH 7.5) to yield a 40 mM stock solution. Incubation conditions were optimized for linearity with respect to time, substrate concentration, and protein concentration based on a previous report (Uchaipichat et al., 2004).

**Initial Testing.** Incubation mixtures (150  $\mu$ L total volume) consisted of HIMs (0.2 mg/mL), HLMs (0.4 mg/mL), or UGT1A-overexpressing HEK293 cell lysates (0.05, 0.025, or 0.02 mg/mL for UGT1A1, UGT1A8, and UGT1A10, respectively); 4-MU [100 (HIMs, HLMs) or 75 (HEK293 lysates)  $\mu$ M]; dietary constituent (10 or 100  $\mu$ M) or the prototypic UGT inhibitor nicardipine (400  $\mu$ M) (Lapham et al., 2012); BSA (0.05%); alamethicin (50  $\mu$ g/mg protein; mixtures containing HIMs and cell lysates); saccharolactone (100  $\mu$ M); and Tris-HCl buffer supplemented with magnesium chloride (5 mM). The selected dietary constituent concentrations were based on a reasonable approximation of the anticipated range of concentrations in the gut (Brantley et al., 2010; Brantley et al., 2013) and were used to plan subsequent  $IC_{50}$  determination experiments (see below). HIMs and cell lysates were activated by incubating with alamethicin on ice for 15 min. Mixtures were equilibrated at 37°C for 10 min before initiating the reactions with UDPGA (4 mM final concentration). 4-MU depletion was monitored via fluorescence (365 nm excitation, 450 nm emission) at pre-determined intervals from 0-20 min with a Synergy H1M monochromator-based multimode microplate reader (BioTek, Winooski, VT). 4-MU concentrations were quantified using Gen5™ data analysis software (v2.0, BioTek) by interpolation from matrix-matched calibration curves. Measurement time intervals were optimized for each protein source to capture the linear phase of 4-MU depletion and to minimize incubation times (data not shown).

**Apparent  $IC_{50}$  Determination.** Constituents/extracts demonstrating >50% inhibition at 100  $\mu$ M (microsomes) or 10  $\mu$ M (cell lysates) were selected for  $IC_{50}$  determination. Incubation conditions mirrored those detailed for initial testing except a range of inhibitor concentrations



(n=7) was tested. The prototypic UGT inhibitors diclofenac and nifedipine were included as comparators. Initial estimates were determined by visual inspection of the velocity of 4-MU depletion versus the natural logarithm of inhibitor concentration. Final parameter estimates were recovered by fitting eq. 1, 2 (DeLean et al., 1978), or 3 (Pietsch et al., 2009) to untransformed data via nonlinear least squares regression using Phoenix<sup>®</sup> WinNonlin<sup>®</sup> (v.6.3, Certara, St Louis, MO):

$$v = \frac{v_0}{1 + \left(\frac{I}{IC_{50}}\right)} \quad (1)$$

$$v = \frac{v_0}{1 + \left(\frac{I}{IC_{50}}\right)^h} \quad (2)$$

$$v = \frac{v_0 - v_{min}}{\left(1 + \left(\frac{I}{IC_{50}}\right)^h\right) + v_{min}} \quad (3)$$

where  $v$  denotes the velocity of 4-MU depletion,  $v_0$  denotes the initial velocity of 4-MU depletion in the absence of inhibitor,  $I$  denotes the nominal inhibitor concentration,  $h$  denotes the Hill coefficient, and  $v_{min}$  denotes the velocity of 4-MU depletion in the presence of infinite inhibitor concentration. The best-fit equation was determined by visual inspection of the observed versus predicted data, randomness of the residuals, Akaike information criteria, and S.E.'s of the parameter estimates.

### **Silybin A, Silybin B, and Silibinin Microsomal Intrinsic Clearance Determination**

Rapid clearance of dietary substance constituents may impact the determination of UGT inhibition potency. Silibinin, a semi-purified milk thistle extract composed of a 1:1 mixture of silybin A and silybin B (Kroll et al., 2007), was selected previously as a model herbal product perpetrator of dietary substance-drug interactions (Brantley et al., 2013; Brantley et al., 2014b).

Microsomal intrinsic clearances of silybin A and silybin B were determined to assess the impact of inhibitor depletion on the recovery of apparent  $IC_{50}$  using pooled HIMs and HLMs.

**Microsomal Incubations.** Conditions mirrored those described above. Silybin A and silybin B concentration ranges encompassing the  $K_m$  or  $S_{50}$  (estimated from the  $IC_{50}$ ) for each enzyme source were used to recover kinetic parameters ( $K_m$  or  $S_{50}$ ,  $V_{max}$ ) via the multiple depletion curves method (Sjogren et al., 2009). Silybin A and silybin B concentration was measured at seven pre-defined time points from triplicate incubations of six initial concentrations. Reactions were initiated by addition of UDPGA (4 mM) and terminated at pre-determined intervals by removing 100  $\mu$ L from the incubation and diluting into 300  $\mu$ L of ice-cold methanol containing internal standard (naringin, 1  $\mu$ M). Samples were centrifuged (3000 g, 10 min, 4°C), and 125  $\mu$ L of supernatant were removed and transferred to clean 96-well plates for analysis by UHPLC-MS/MS.

**Quantification of Silybin A and Silybin B by UHPLC-MS/MS.** Chromatographic separation was achieved using an HSS T3 column (1.8  $\mu$ M, 2.1 x 100 mm) with a Vanguard Pre-Column (2.1 x 5 mm) (Waters Corporation, Waltham, MA) heated to 50°C and a binary gradient at a flow rate of 0.6 mL/min. The gradient elution started at 70:30 water:methanol (each with 0.1% formic acid) and increased linearly to 45:55 of phase A to B over 5 min before returning to initial conditions over 0.1 min and holding for 0.9 min; the total run time was 6 min. Samples were analyzed (3  $\mu$ L injection volume) using the QTRAP<sup>®</sup> 6500 UHPLC-MS/MS system (AB Sciex, Framingham, MA) with turbo electrospray source operated in negative ion mode. The declustering potential and collision energy were set at -25 V and -32 mV, respectively. Silybin A and silybin B (481.1→125.1 m/z), monoglucuronide conjugates (657.1→481.1 m/z), and naringin (579.0→271.0 m/z) were monitored in multiple reaction monitoring mode. Silybin A and silybin B concentrations were quantified using MultiQuant<sup>™</sup> software (v2.1.1, AB Sciex) by interpolation from matrix matched calibration curves and quality controls with a linear range of 0.8-200  $\mu$ M. The calibration standards and quality controls were

judged for batch quality based on the 2013 FDA guidance for industry regarding bioanalytical method validation (Food and Drug Administration Center for Drug Evaluation and Research, 2013). Peak area ratios were used to assess glucuronide formation qualitatively, as authentic standards were not available.

**Calculation of Intrinsic Clearance.**  $K_m$  or  $S_{50}$  and  $V_{max}$  were obtained by fitting the simple Michaelis-Menten (eq. 4) or Hill (eq. 5) equation to [substrate] versus depletion velocity data using Phoenix<sup>®</sup> WinNonlin<sup>®</sup>:

$$v = \frac{V_{max} \times [S]}{K_m + [S]} \quad (4)$$

$$v = \frac{V_{max} \times [S]^h}{S_{50}^h + [S]^h} \quad (5)$$

where  $v$  denotes the velocity of substrate depletion,  $S$  denotes nominal substrate concentration, and  $S_{50}$  denotes the substrate concentration corresponding to 50% of  $V_{max}$ .

### Impact of Inhibitor Depletion on Apparent $IC_{50}$ Determination

The apparent  $IC_{50}$ s were recovered initially using nominal inhibitor concentration as described above. The impact of inhibitor depletion was determined using predicted inhibitor concentrations present at each time point during the 20 min incubation period. Inhibitor depletion at each concentration was described by eq. 6:

$$V \times \frac{dC_{inh}}{dt} = -Cl_{int} \times C_{inh} \quad (6)$$

where  $V$  is the volume of the incubation per milligram of microsomal protein,  $C_{inh}$  is the concentration of inhibitor in the incubation,  $t$  is time, and  $Cl_{int}$  is the intrinsic clearance of the inhibitor calculated as the ratio of  $V_{max}$  to  $K_m$ .  $Cl_{max}$  was calculated for an inhibitor described by the Hill equation using eq. 7 (Houston and Kenworthy, 2000) and input into eq. 6 in place of  $Cl_{int}$ :

$$C_{I_{\max}} = \frac{V_{\max} \times (h-1)}{S_{50} + h(h-1)^{1/h}} \quad (7)$$

Model equations were input into Phoenix<sup>®</sup> WinNonlin<sup>®</sup>. The fold IC<sub>50</sub> shift was calculated as the ratio of the apparent IC<sub>50</sub> using nominal concentration to the shifted IC<sub>50</sub> using predicted inhibitor concentrations at 10 or 20 min.

### Statistical Analysis

Data are presented as means ± S.D.'s of triplicate incubations unless indicated otherwise. IC<sub>50</sub>s are presented as the estimates ± S.E.'s. Concentration-dependent inhibition was evaluated by a paired Student's *t*-test using untransformed data. A *p*<0.05 was considered significant.

## Results

**Diet-derived constituents differentially inhibit intestinal 4-MU glucuronidation.** All dietary constituents/extracts inhibited 4-MU glucuronidation in a concentration-dependent manner (10 versus 100  $\mu$ M) in HIMs (with the exception of isosilybin A) (Fig. 1A, B) and in HLMS (Fig. 1C, D). Constituents/extracts that inhibited activity by >50% at 100  $\mu$ M relative to vehicle were selected for  $IC_{50}$  determination (HIMs: silybin A, silybin B, isosilybin B, silymarin, kaempferol, quercetin, EGCG; HLMS: silybin B, silymarin, kaempferol, quercetin, EGCG). Compared to the UGT activity in HIMs and HLMS, activity in UGT1A-overexpressing HEK293 cell lysates was generally more sensitive to inhibition by the tested constituents/extracts, particularly the milk thistle flavonolignans towards UGT1A8 (Fig. 2). The lack of concentration-dependent inhibition by several constituents/extracts reflected potent inhibition (>50%) at 10  $\mu$ M and minimal changes in 4-MU depletion rate at 100  $\mu$ M, a sensitivity limitation inherent to the substrate depletion method. Constituents/extracts that inhibited 4-MU glucuronidation by >50% at 10  $\mu$ M for individual UGTs were selected for  $IC_{50}$  determination [UGT1A1: silybin A, isosilybin B, isosilychristin, silydianin, silibinin, naringin, kaempferol, EGCG (Fig. 2A, B); UGT1A8: silybin A, silybin B, isosilybin A, isosilybin B, silychristin, isosilychristin, silydianin, silibinin, silymarin, naringin, kaempferol (Fig. 2C, D); UGT1A10: silybin A, isosilybin B, silychristin, silydianin, naringin, naringenin, kaempferol, quercetin (Fig. 2E, F)]. Silybin B also was selected for testing with UGT1A1 based on its contribution to silibinin composition (Kroll et al., 2007).

**Diet-derived constituents inhibit intestinal UGTs at clinically achievable concentrations.** The  $IC_{50}$  of the majority of the constituents/extracts (13 of 15) was  $\leq 10$   $\mu$ M with at least one enzyme source (Table 1). Intestinal microsomal activity was more sensitive to inhibition than hepatic microsomal activity; the  $IC_{50}$  for silybin B, silymarin, kaempferol, quercetin, and EGCG was lower with HIMs than with HLMS. Kaempferol was the most potent inhibitor of UGT activity in both HIMs and HLMS. The  $IC_{50}$ s of all constituents towards UGT1A8 and UGT1A10 activity were <11  $\mu$ M. Silydianin was the most potent inhibitor of both UGT1A1

and UGT1A8 activity, whereas kaempferol was the most potent inhibitor of UGT1A10 activity. Dietary constituents/extracts were more potent than prototypic drug inhibitors, consistent with a previous report (Uchaipichat et al., 2004). The  $IC_{50}$  of diclofenac with HLMs was described best by eq. 3, indicating a lack of inhibitory potency towards one or more isoforms catalyzing 4-MU glucuronidation.

**The multiple depletion curves method enabled recovery of silybin A and silybin B microsomal intrinsic clearance parameters.** UHPLC separation coupled with the AB SCIEX QTRAP<sup>®</sup> 6500 platform facilitated rapid separation (6 min total run time) and sensitive detection (lower limit of quantitation, 0.8  $\mu$ M) of silybin A, silybin B, and respective monoglucuronides (Fig. 3). Silybin A and silybin B were cleared rapidly by both HIMs and HLMs. Silybin A glucuronidation by HIMs was described best by the Hill equation (eq. 5), whereas glucuronidation by HLMs was described best by the simple Michaelis-Menten equation (eq. 4) (Table 2, Fig. 4A). Silybin B glucuronidation by both HIMs and HLMs was described best by the simple Michaelis-Menten equation (Table 2, Fig. 4B, C). Solubility limitations with silybin B precluded use of higher substrate concentrations for accurate recovery of  $V_{max}$  (Fig. 4). Qualitative assessment of glucuronide formation indicated two monoglucuronide metabolites for both silybin A and silybin B (Fig. 3). Both compounds appeared to generate one metabolite (monoglucuronide 1) with higher affinity than the other (monoglucuronide 2), consistent with a previous report of regioselective silibinin metabolism (Jancova et al., 2011) (Table 2, Fig. 5).

**Inhibitor depletion can impact apparent  $IC_{50}$  determination for rapidly cleared UGT inhibitors.** Relatively slow clearance of silybin A by HIMs resulted in minimal changes in  $IC_{50}$  (<1.1-fold shift at 10 and 20 min, respectively) (Fig. 6, A). The  $IC_{50}$  of silybin B with HIMs shifted 1.3- and 1.9-fold at 10 and 20 min, respectively (Fig. 6, B). The ~1.5-fold more rapid clearance of silybin B by HLMs (compared to silybin B by HIMs) resulted in a 1.6- and 2.8-fold shift in  $IC_{50}$  at 10 and 20 min, respectively (Fig. 6, C).

## Discussion

Clinicians and consumers are becoming increasingly aware of the potential for interactions between diet-derived substances and conventional medications. However, definitive evidence supporting the risk or safety of certain dietary substance-drug combinations remains scarce. This deficiency is due in part to the complex composition of dietary substances, precluding application of established paradigms used to assess drug-drug interaction risk. A working framework to elucidate potential mechanisms underlying dietary substance-drug interactions has been proposed (National Center for Complementary and Alternative Medicine, 2012; Won et al., 2012; Brantley et al., 2013; Brantley et al., 2014a; Brantley et al., 2014b). This framework centers on the evaluation of isolated constituents to ascertain the relative contribution of each constituent to the mixture, as well as to identify marker constituents that can be used to predict the likelihood and magnitude of these interactions. As an extension of previous studies focused on CYP-mediated inhibition (Brantley et al., 2010; Kim et al., 2011; Brantley et al., 2013; Brantley et al., 2014b), this framework was applied to 13 isolated constituents and two extracts as inhibitors of glucuronidation with a focus on gut-relevant enzymes.

Initial testing, involving two concentrations (10, 100  $\mu\text{M}$ ) of each constituent/extract, demonstrated HIMs and HEK293 cell lysates overexpressing gut-relevant UGT1A isoforms (UGT1A1, UGT1A8, and UGT1A10) to be more sensitive to inhibition than HLMs (Figs. 1, 2). Dietary substance-drug interactions mediated via inhibition of hepatic UGT1A have been deemed unlikely based on in vitro inhibition constants ( $K_s$ ,  $IC_{50s}$ ) of selected individual constituents that were well above maximum plasma concentrations ( $C_{max}$ ) observed in human pharmacokinetic studies ( $\mu\text{M}$  versus  $\text{nM}$ ) (Mohamed and Frye, 2011a; Gurley et al., 2012; Li et al., 2012). Clinical evaluation of diet-derived substances as inhibitors of systemic drug glucuronidation, including garlic (Gwilt et al., 1994) and milk thistle (van Erp et al., 2005), confirmed minimal or no interaction risk with the UGT1A substrates acetaminophen and

irinotecan, respectively. Consistent with previous reports, the  $IC_{50}$ s obtained with HLMs in the current work exceeded maximum systemic concentrations typically observed in vivo for milk thistle flavonolignans, kaempferol, quercetin, or EGCG ( $>25 \mu\text{M}$  versus  $\leq 1 \mu\text{M}$ ) (Manach et al., 2005; Ude et al., 2013; Zhu et al., 2013). These data reinforce the assertion that diet-derived constituents are unlikely to perpetrate clinically relevant interactions with conventional medications via inhibition of hepatic UGTs. However, nanoparticle formulations (Nair et al., 2010), pro-drug strategies (Biasutto and Zoratti, 2014), phytosome complexes (Kidd, 2009), and other approaches to enhance systemic exposure of diet-derived constituents may alter future interpretation.

Compared to the liver, the intestine does not express the same complement of UGTs in terms of both abundance and isoform diversity (Court et al., 2012; Fallon et al., 2013), which may explain why HIMs were more sensitive to inhibition by diet-derived substances than HLMs. Initial testing with HEK293 cell lysates showed that UGT1A8 and UGT1A10 were the most sensitive to inhibition by diet-derived constituents/extracts, suggesting that drug substrates for these isoforms may carry increased risk of interactions mediated by inhibition of enteric glucuronidation. Based on a predefined criterion of  $>50\%$  inhibition of UGT activity in any enzyme source (Figs. 1 and 2), 14 constituents/extracts were selected for  $IC_{50}$  determination.

The  $IC_{50}$ s of the milk thistle flavonolignans and extracts, naringin, naringenin, kaempferol, and quercetin towards intestinal UGT activity (Table 1) were well below concentrations measured in intestinal tissue or citrus juices. For example, the  $IC_{50}$ s of silibinin and isolated constituents silybin A and silybin B ( $<10 \mu\text{M}$ ) were more than 10x lower than mean colorectal tissue concentrations following oral administration of 1400 mg silibinin to cancer patients ( $\sim 140 \mu\text{M}$ ) (Hoh et al., 2006). Likewise, the  $IC_{50}$ s of naringin and naringenin ( $<10 \mu\text{M}$ ) were at least 30x lower than concentrations in citrus juices ( $>300 \mu\text{M}$ ) (Erlund et al., 2001; Vandermolen et al., 2013). Finally, the  $IC_{50}$ s of kaempferol and quercetin, which are present in myriad foods, were below estimated concentrations in the intestinal lumen ( $<10 \mu\text{M}$  versus 15-



20  $\mu\text{M}$ ) (Mohamed and Frye, 2010). Potent inhibition of enteric UGTs by these constituents/extracts at clinically achievable intestinal concentrations warrant further evaluation as potential perpetrators of clinically relevant dietary substance-drug interactions via dynamic pharmacokinetic modeling and simulation techniques (Food and Drug Administration Center for Drug Evaluation and Research, 2012; Won et al., 2012; Brantley et al., 2014b) .

UGT1A-overexpressing HEK293 cell lysates enabled investigation of isoform selective inhibition using a non-selective probe substrate to provide additional insight into inhibitory behavior observed with pooled microsomes. For example, kaempferol was shown previously to inhibit glucuronidation of the immunosuppressant mycophenolic acid (MPA) by both HLMs and HLMS, with a  $K_i$  of  $4.5 \pm 1.2$  and  $33.6 \pm 2.5$   $\mu\text{M}$ , respectively (Mohamed and Frye, 2010). Inhibition of activity in HLMS could be attributed to inhibition of UGT1A9, as MPA is believed to be a UGT1A9 selective probe in HLMS (Court, 2005). The isoforms associated with inhibition of MPA glucuronidation in HLMs may include UGT1A8 and 1A10, which are expressed in intestinal tissue (Tukey and Strassburg, 2000) and known to catalyze the metabolism of MPA in vitro (Picard et al., 2005). The potent inhibition of UGT1A8 and 1A10 by kaempferol observed in the current work ( $\text{IC}_{50}$ ,  $0.9 \pm 0.4$  and  $10.6 \pm 1.6$   $\mu\text{M}$ , respectively) supports this contention.

Clinically relevant intestinal UGT substrates include the anti-cancer agent, raloxifene, and the cholesterol lowering agent, ezetimibe (Kemp et al., 2002; Ghosal et al., 2004; Sun et al., 2013). Raloxifene intestinal glucuronidation is catalyzed predominately by both UGT1A8 and UGT1A10 (Sun et al., 2013). Inhibition of these enzymes could increase raloxifene bioavailability, increasing systemic exposure and the risk of adverse effects, including hot flashes and venous thromboembolism. Conversely, inhibition of intestinal glucuronidation could attenuate formation of the pharmacologically active glucuronide of ezetimibe, reducing therapeutic efficacy. Ezetimibe glucuronidation is mediated by multiple UGTs, including members of both the UGT1A and UGT2B families (Ghosal et al., 2004). Structure-activity relationships suggest that compounds containing the flavonol backbone, a common structural

feature of many diet-derived constituents, are candidate substrates and inhibitors of the UGT1A family (Tripathi et al., 2013). Potent inhibition of intestinal UGT1As by dietary substances may impact the in vivo disposition of ezetimibe, but the potential exists for compensation by other UGTs, including UGT2B7 and UGT2B15. Although not investigated in the current work, diet-derived constituents may be potent inhibitors of these isoforms, particularly constituents containing a steroidal backbone, such as the saponins present in ginseng preparations (Fang et al., 2013). This observation raises the possibility of dietary substance-drug interactions mediated by inhibition of intestinal UGT2B7 and UGT2B15.

The immense chemical diversity of diet-derived constituents and the potential for interactions mediated via inhibition of several UGT isoforms highlight the need for an efficient and systematic approach to identify candidate inhibitors for further evaluation. A plate reader-based assay involving the non-specific UGT probe substrate, 4-MU, and pooled microsomal and isoform-specific enzyme systems was used as cost-effective means to screen multiple diet-derived constituents/extracts as inhibitors of intestinal glucuronidation and prioritize for further investigation. This assay enabled real-time kinetic measurement of substrate depletion and eliminated the need for extended incubation times. Short incubation times should minimize artifacts due to excessive (>20%) inhibitor or substrate depletion, as well as reduce the potential inhibition by UDP generated by these processes (Fujiwara et al., 2008). The impact of inhibitor depletion on the apparent  $IC_{50}$  recovered for an exemplar diet-derived constituent, silybin B, with HLMs (Fig. 6, C) further highlights the importance of minimizing incubation times. Results imply that using nominal inhibitor concentrations may underpredict the potency of rapidly cleared inhibitors, resulting in a less conservative estimate of interaction risk. Such an underprediction may be concerning while interpreting screening data when inhibitors are binned into risk categories based on apparent  $IC_{50}$ s recovered using nominal concentrations. UGT substrates, especially polyphenolic diet-derived constituents, tend to be cleared rapidly, making

consideration of inhibitor depletion (in addition to substrate depletion) particularly important when evaluating candidate UGT inhibitors.

In summary, using a time- and cost-efficient assay, multiple diet-derived constituents/extracts from structurally diverse chemical classes were identified as potent inhibitors of intestinal UGT1A isoforms, particularly UGT1A8 and UGT1A10. Although inhibition potency towards 4-MU glucuronidation may not be predictive of the effects on enteric glucuronidation of clinically relevant substrates (Dong et al., 2012; Chengcheng et al., 2013), these dietary substances could be evaluated further as inhibitors of such substrates, including ezetimibe, mycophenolic acid, and raloxifene, using a similar systematic approach. Results would prioritize for advanced modeling and simulation techniques that integrate in vitro inhibitory potency ( $K_i$ ) with available clinical pharmacokinetic data to provide quantitative predictions of dietary substance-drug interaction risk (Brantley et al., 2014b). Modeling and simulation can be used to prioritize for clinical evaluation and to guide the design of clinical interaction studies, with the ultimate goal of providing conclusive evidence about the risk or safety of certain dietary substance-drug combinations.

## **Acknowledgements**

M.F.P. dedicates this article to Dr. David P. Paine.

### **Authorship Contributions**

Participated in research design: Gufford, Paine, Lazarus

Conducted experiments: Gufford

Contributed new reagents or analytical tools: Graf, Oberlies, Lazarus, Chen

Performed data analysis: Gufford, Paine

Wrote or contributed to writing of the manuscript: Gufford, Graf, Chen, Lazarus, Oberlies, Paine

## References

- Bailey DG, Dresser G, and Arnold JM (2013) Grapefruit-medication interactions: forbidden fruit or avoidable consequences? *CMAJ* **185**:309-316.
- Biasutto L and Zoratti M (2014) Prodrugs of quercetin and resveratrol: a strategy under development. *Curr Drug Metab* **15**:77-95.
- Brantley SJ, Argikar AA, Lin YS, Nagar S, and Paine MF (2014a) Herb-drug interactions: challenges and opportunities for improved predictions. *Drug Metab Dispos* **42**:301-317.
- Brantley SJ, Graf TN, Oberlies NH, and Paine MF (2013) A systematic approach to evaluate herb-drug interaction mechanisms: investigation of milk thistle extracts and eight isolated constituents as CYP3A inhibitors. *Drug Metab Dispos* **41**:1662-1670.
- Brantley SJ, Gufford BT, Dua R, Fediuk DJ, Graf TN, Scarlett YV, Frederick KS, Fisher MB, Oberlies NH, and Paine MF (2014b) Physiologically based pharmacokinetic modeling framework for quantitative prediction of an herb-drug interaction. *CPT Pharmacometrics Syst Pharmacol* **3**:e107.
- Brantley SJ, Oberlies NH, Kroll DJ, and Paine MF (2010) Two flavonolignans from milk thistle (*Silybum marianum*) inhibit CYP2C9-mediated warfarin metabolism at clinically achievable concentrations. *J Pharmacol Exp Ther* **332**:1081-1087.
- Chengcheng G, Rui X, Tianheng M, Wei Y, and Liqun P (2013) Probe substrate and enzyme source-dependent inhibition of UDP-glucuronosyltransferase (UGT) 1A9 by wogonin. *Afr Health Sci* **13**:551-555.
- Court MH (2005) Isoform-selective probe substrates for in vitro studies of human UDP-glucuronosyltransferases. *Methods Enzymol* **400**:104-116.
- Court MH, Zhang X, Ding X, Yee KK, Hesse LM, and Finel M (2012) Quantitative distribution of mRNAs encoding the 19 human UDP-glucuronosyltransferase enzymes in 26 adult and 3 fetal tissues. *Xenobiotica* **42**:266-277.
- Davis-Searles PR, Nakanishi Y, Kim NC, Graf TN, Oberlies NH, Wani MC, Wall ME, Agarwal R, and Kroll DJ (2005) Milk thistle and prostate cancer: differential effects of pure flavonolignans from *Silybum marianum* on antiproliferative end points in human prostate carcinoma cells. *Cancer Res* **65**:4448-4457.
- DeLean A, Munson PJ, and Rodbard D (1978) Simultaneous analysis of families of sigmoidal curves: application to bioassay, radioligand assay, and physiological dose-response curves. *Am J Physiol* **235**:E97-102.
- Dong RH, Fang ZZ, Zhu LL, Liang SC, Ge GB, Yang L, and Liu ZY (2012) Investigation of UDP-glucuronosyltransferases (UGTs) inhibitory properties of carvacrol. *Phytother Res* **26**:86-90.
- Erlund I, Meririnne E, Alfthan G, and Aro A (2001) Plasma kinetics and urinary excretion of the flavanones naringenin and hesperetin in humans after ingestion of orange juice and grapefruit juice. *J Nutr* **131**:235-241.
- Fallon JK, Neubert H, Goosen TC, and Smith PC (2013) Targeted precise quantification of 12 human recombinant uridine-diphosphate glucuronosyl transferase 1A and 2B isoforms using nano-ultra-high-performance liquid chromatography/tandem mass spectrometry with selected reaction monitoring. *Drug Metab Dispos* **41**:2076-2080.
- Fang ZZ, Cao YF, Hu CM, Hong M, Sun XY, Ge GB, Liu Y, Zhang YY, Yang L, and Sun HZ (2013) Structure-inhibition relationship of ginsenosides towards UDP-glucuronosyltransferases (UGTs). *Toxicol Appl Pharmacol* **267**:149-154.
- Food and Drug Administration Center for Drug Evaluation and Research (2012) Drug interaction studies - study design, data analysis, implications for dosing, and labeling recommendations (draft guidance).
- Food and Drug Administration Center for Drug Evaluation and Research (2013) Bioanalytical method validation (draft guidance).

- Fujiwara R, Nakajima M, Yamanaka H, Katoh M, and Yokoi T (2008) Product inhibition of UDP-glucuronosyltransferase (UGT) enzymes by UDP obfuscates the inhibitory effects of UGT substrates. *Drug Metab Dispos* **36**:361-367.
- Ghosal A, Hapangama N, Yuan Y, Achanfuo-Yeboah J, Iannucci R, Chowdhury S, Alton K, Patrick JE, and Zbaida S (2004) Identification of human UDP-glucuronosyltransferase enzyme(s) responsible for the glucuronidation of ezetimibe (Zetia). *Drug Metab Dispos* **32**:314-320.
- Graf TN, Wani MC, Agarwal R, Kroll DJ, and Oberlies NH (2007) Gram-scale purification of flavonolignan diastereoisomers from *Silybum marianum* (Milk Thistle) extract in support of preclinical in vivo studies for prostate cancer chemoprevention. *Planta Med* **73**:1495-1501.
- Gurley BJ, Fifer EK, and Gardner Z (2012) Pharmacokinetic herb-drug interactions (part 2): drug interactions involving popular botanical dietary supplements and their clinical relevance. *Planta Med* **78**:1490-1514.
- Gwilt PR, Lear CL, Tempero MA, Birt DD, Grandjean AC, Ruddon RW, and Nagel DL (1994) The effect of garlic extract on human metabolism of acetaminophen. *Cancer Epidemiol Biomarkers Prev* **3**:155-160.
- Hoh C, Boocock D, Marczylo T, Singh R, Berry DP, Dennison AR, Hemingway D, Miller A, West K, Euden S, Garcea G, Farmer PB, Steward WP, and Gescher AJ (2006) Pilot study of oral silibinin, a putative chemopreventive agent, in colorectal cancer patients: silibinin levels in plasma, colorectum, and liver and their pharmacodynamic consequences. *Clin Cancer Res* **12**:2944-2950.
- Houston JB and Kenworthy KE (2000) In vitro-in vivo scaling of CYP kinetic data not consistent with the classical Michaelis-Menten model. *Drug Metab Dispos* **28**:246-254.
- Jancova P, Siller M, Anzenbacherova E, Kren V, Anzenbacher P, and Simanek V (2011) Evidence for differences in regioselective and stereoselective glucuronidation of silybin diastereomers from milk thistle (*Silybum marianum*) by human UDP-glucuronosyltransferases. *Xenobiotica* **41**:743-751.
- Kemp DC, Fan PW, and Stevens JC (2002) Characterization of raloxifene glucuronidation in vitro: contribution of intestinal metabolism to presystemic clearance. *Drug Metab Dispos* **30**:694-700.
- Kiang TK, Ensom MH, and Chang TK (2005) UDP-glucuronosyltransferases and clinical drug-drug interactions. *Pharmacol Ther* **106**:97-132.
- Kidd PM (2009) Bioavailability and activity of phytosome complexes from botanical polyphenols: the silymarin, curcumin, green tea, and grape seed extracts. *Altern Med Rev* **14**:226-246.
- Kim E, Sy-Cordero A, Graf TN, Brantley SJ, Paine MF, and Oberlies NH (2011) Isolation and identification of intestinal CYP3A inhibitors from cranberry (*Vaccinium macrocarpon*) using human intestinal microsomes. *Planta Med* **77**:265-270.
- Kroll DJ, Shaw HS, and Oberlies NH (2007) Milk thistle nomenclature: why it matters in cancer research and pharmacokinetic studies. *Integr Cancer Ther* **6**:110-119.
- Lapham K, Bauman JN, Walsky RL, Niosi M, Orozco CC, Bourcier K, Giddens G, Obach RS, and Hyland R (2012) Digoxin and tranilast as novel isoform selective inhibitors of human UDP glucuronosyltransferase 1A9. *Drug Metabolism Reviews* **44**:36-152.
- Li L, Hu H, Xu S, Zhou Q, and Zeng S (2012) Roles of UDP-glucuronosyltransferases in phytochemical metabolism of herbal medicines and the associated herb-drug interactions. *Curr Drug Metab* **13**:615-623.
- Manach C, Williamson G, Morand C, Scalbert A, and Remesy C (2005) Bioavailability and bioefficacy of polyphenols in humans. I. Review of 97 bioavailability studies. *Am J Clin Nutr* **81**:230S-242S.

- Mohamed ME and Frye RF (2011a) Effects of herbal supplements on drug glucuronidation. Review of clinical, animal, and in vitro studies. *Planta Med* **77**:311-321.
- Mohamed ME and Frye RF (2011b) Inhibitory effects of commonly used herbal extracts on UDP-glucuronosyltransferase 1A4, 1A6, and 1A9 enzyme activities. *Drug Metab Dispos* **39**:1522-1528.
- Mohamed MF and Frye RF (2010) Inhibition of intestinal and hepatic glucuronidation of mycophenolic acid by Ginkgo biloba extract and flavonoids. *Drug Metab Dispos* **38**:270-275.
- Mohamed MF, Tseng T, and Frye RF (2010) Inhibitory effects of commonly used herbal extracts on UGT1A1 enzyme activity. *Xenobiotica* **40**:663-669.
- Nair HB, Sung B, Yadav VR, Kannappan R, Chaturvedi MM, and Aggarwal BB (2010) Delivery of antiinflammatory nutraceuticals by nanoparticles for the prevention and treatment of cancer. *Biochem Pharmacol* **80**:1833-1843.
- Napolitano JG, Lankin DC, Graf TN, Friesen JB, Chen SN, McAlpine JB, Oberlies NH, and Pauli GF (2013) HiFSA fingerprinting applied to isomers with near-identical NMR spectra: the silybin/isosilybin case. *J Org Chem* **78**:2827-2839.
- National Center for Complementary and Alternative Medicine (2012) Summary of roundtable meeting on dietary supplement-drug interactions.
- Paine MF and Oberlies NH (2007) Clinical relevance of the small intestine as an organ of drug elimination: drug-fruit juice interactions. *Expert Opin Drug Metab Toxicol* **3**:67-80.
- Picard N, Ratanasavanh D, Premaud A, Le Meur Y, and Marquet P (2005) Identification of the UDP-glucuronosyltransferase isoforms involved in mycophenolic acid phase II metabolism. *Drug Metab Dispos* **33**:139-146.
- Pietsch M, Christian L, Inhester T, Petzold S, and Gutschow M (2009) Kinetics of inhibition of acetylcholinesterase in the presence of acetonitrile. *FEBS J* **276**:2292-2307.
- Ritter JK (2007) Intestinal UGTs as potential modifiers of pharmacokinetics and biological responses to drugs and xenobiotics. *Expert Opin Drug Metab Toxicol* **3**:93-107.
- Sjogren E, Lennernas H, Andersson TB, Grasjo J, and Bredberg U (2009) The multiple depletion curves method provides accurate estimates of intrinsic clearance (CL<sub>int</sub>), maximum velocity of the metabolic reaction (V<sub>max</sub>), and Michaelis constant (K<sub>m</sub>): accuracy and robustness evaluated through experimental data and Monte Carlo simulations. *Drug Metab Dispos* **37**:47-58.
- Sun D, Jones NR, Manni A, and Lazarus P (2013) Characterization of raloxifene glucuronidation: potential role of UGT1A8 genotype on raloxifene metabolism in vivo. *Cancer Prev Res (Phila)* **6**:719-730.
- Tripathi SP, Bhadauriya A, Patil A, and Sangamwar AT (2013) Substrate selectivity of human intestinal UDP-glucuronosyltransferases (UGTs): in silico and in vitro insights. *Drug Metab Rev* **45**:231-252.
- Tukey RH and Strassburg CP (2000) Human UDP-glucuronosyltransferases: metabolism, expression, and disease. *Annu Rev Pharmacol Toxicol* **40**:581-616.
- Uchaipichat V, Mackenzie PI, Guo XH, Gardner-Stephen D, Galetin A, Houston JB, and Miners JO (2004) Human udp-glucuronosyltransferases: isoform selectivity and kinetics of 4-methylumbelliferone and 1-naphthol glucuronidation, effects of organic solvents, and inhibition by diclofenac and probenecid. *Drug Metab Dispos* **32**:413-423.
- Ude C, Schubert-Zsilavec M, and Wurglics M (2013) Ginkgo biloba extracts: a review of the pharmacokinetics of the active ingredients. *Clin Pharmacokinet* **52**:727-749.
- van Erp NP, Baker SD, Zhao M, Rudek MA, Guchelaar HJ, Nortier JW, Sparreboom A, and Gelderblom H (2005) Effect of milk thistle (*Silybum marianum*) on the pharmacokinetics of irinotecan. *Clin Cancer Res* **11**:7800-7806.



- Vandermolen KM, Cech NB, Paine MF, and Oberlies NH (2013) Rapid Quantitation of Furanocoumarins and Flavonoids in Grapefruit Juice using Ultra-Performance Liquid Chromatography. *Phytochem Anal* **24**:654-660.
- Williams JA, Hyland R, Jones BC, Smith DA, Hurst S, Goosen TC, Peterkin V, Koup JR, and Ball SE (2004) Drug-drug interactions for UDP-glucuronosyltransferase substrates: a pharmacokinetic explanation for typically observed low exposure (AUC<sub>i</sub>/AUC) ratios. *Drug Metab Dispos* **32**:1201-1208.
- Won CS, Oberlies NH, and Paine MF (2012) Mechanisms underlying food-drug interactions: inhibition of intestinal metabolism and transport. *Pharmacol Ther* **136**:186-201.
- Wu B, Kulkarni K, Basu S, Zhang S, and Hu M (2011) First-pass metabolism via UDP-glucuronosyltransferase: a barrier to oral bioavailability of phenolics. *J Pharm Sci* **100**:3655-3681.
- Zhu HJ, Brinda BJ, Chavin KD, Bernstein HJ, Patrick KS, and Markowitz JS (2013) An assessment of pharmacokinetics and antioxidant activity of free silymarin flavonolignans in healthy volunteers: a dose escalation study. *Drug Metab Dispos* **41**:1679-1685.

## Footnotes

a. This work was supported by the National Institutes of Health National Institute of General Medical Sciences [Grant R01 GM077482-S1]. B.T.G. was supported by a fellowship awarded by the American Foundation for Pharmaceutical Education.

b. Reprint requests: Mary F. Paine, RPh, PhD

PBS 341, PO Box 1495

College of Pharmacy

Washington State University

Spokane, WA 99210-1495

Office: (509) 358-7759

Fax: (509) 368-6561

Email: mary.paine@wsu.edu

## Figure Legends

**Fig. 1.** Initial testing of milk thistle flavonolignans and other diet-derived constituents as inhibitors of 4-MU glucuronidation in HIMs (A, B) and HLMs (C, D) at 10  $\mu$ M (gray) and 100  $\mu$ M (black) compared to vehicle control (white) (0.1% methanol). Hatched black bars denote the prototypic UGT inhibitor, nocardipine (400  $\mu$ M). Dashed lines denote 50% inhibition. Control activity was  $4.4 \pm 0.5$  and  $12 \pm 0.5$  nmol/min/mg microsomal protein for HIMs and HLMs, respectively. Bars and error bars denote means and SDs, respectively, of triplicate incubations. \* $p < 0.05$ , 10 versus 100  $\mu$ M (paired Student's *t*-test using untransformed data).

**Fig. 2.** Initial testing of milk thistle flavonolignans/extracts and other diet-derived constituents as inhibitors of 4-MU glucuronidation in HEK293 cell lysates overexpressing UGT1A1 (A, B), UGT1A8 (C, D), or UGT1A10 (E, F) at 10  $\mu$ M (gray) and 100  $\mu$ M (black) compared to vehicle control (white) (0.1% methanol). Hatched black bars denote the prototypic UGT inhibitor, nocardipine (400  $\mu$ M). Dashed lines denote 50% inhibition. Control activity was  $13 \pm 1.1$ ,  $20 \pm 5.6$ , and  $56 \pm 7.0$  nmol/min/mg microsomal protein for UGT1A1, UGT1A8, and UGT1A10, respectively. Bars and error bars denote means and SDs, respectively, of triplicate incubations. \* $p < 0.05$ , 10 versus 100  $\mu$ M (paired Student's *t*-test using untransformed data).

**Fig. 3.** Representative UHPLC-MS/MS chromatograms for silybin A (SA, 481.1→125.1 m/z), silybin A monoglucuronides (SA-glucs, 657.1→481.1 m/z), silybin B (SB, 481.1→125.1 m/z), silybin B monoglucuronides (SB-glucs, 657.1→481.1 m/z), and internal standard (IS, 579.0→271.0 m/z). Retention times were 4.6 min (SA), 2.1 min (SA monoglucuronide 1), 2.9 min (SA monoglucuronide 2), 4.8 min (SB), 2.2 min (SB monoglucuronide 1), 3.3 min (SB monoglucuronide 2), and 2.6 min (IS, naringin). A background peak (3.1 min) was consistently present in the glucuronide traces that did not demonstrate time or concentration dependence.

**Fig. 4.** Michaelis-Menten plots for glucuronidation of silybin A (A) and silybin B (B) by HIMs (green) and HLMs (gray) and recovered using the multiple depletion curves method. Symbols

and error bars denote the mean and S.D. of observed values, respectively. Curves denote model-generated values.

**Fig. 5.** Michaelis-Menten plots for glucuronidation of silybin A by HIMs (A) and HLMs (B) and of silybin B by HIMs (C) and HLMs (D) recovered using glucuronide metabolite formation (peak area ratios over time). Monoglucuronide 1 (left column) and monoglucuronide 2 (right column) designations were based on UHPLC retention time. Symbols and error bars denote the mean and S.D. of observed values, respectively. Curves denote model-generated values.

**Fig. 6.** Impact of inhibitor depletion on the recovery of apparent  $IC_{50}$  of silybin A (A) or silybin B (B) by pooled HIMs and of silybin B by pooled HLMs (C). Curves denote nonlinear least-squares regression of observed 4-MU depletion data versus nominal inhibitor concentration (black) or predicted inhibitor concentration at 10 min (dashed) or 20 min (dotted) using Phoenix<sup>®</sup> WinNonlin<sup>®</sup> (version 6.3).

**Table 1.** IC<sub>50</sub> of milk thistle constituents and extracts and other diet-derived constituents towards 4-MU glucuronidation.

	Enzyme Source				
	HLMs	HIMs	UGT1A1	UGT1A8	UGT1A10
<b>Milk Thistle Flavonolignans</b>					
Silybin A	--	64.8 ± 6.3	28.8 ± 5.5	5.9 ± 1.4	2.7 ± 0.6
Silybin B	87.3 ± 7.1	46.9 ± 6.0	27.5 ± 5.7	5.8 ± 1.8	--
Isosilybin A	--	--	--	6.7 ± 1.5	--
Isosilybin B	--	187 ± 30.9	51.1 ± 18.2	7.2 ± 1.4	5.9 ± 0.9
Silychristin	--	--	--	2.5 ± 0.6	6.0 ± 1.1
Isosilychristin	--	--	53.5 ± 15.3	2.0 ± 0.3	--
Silydianin	97.7 ± 8.4	--	5.3 ± 1.7	1.1 ± 0.3	6.8 ± 2.2
<b>Milk Thistle Extracts</b>					
Silibinin	--	--	11.1 ± 3.0	3.9 ± 1.7	--
Silymarin	106 ± 7.0	40.5 ± 5.3	--	4.8 ± 1.6	--
<b>Other Diet-Derived Constituents</b>					
Naringin	--	--	14.8 ± 1.8	6.3 ± 1.3	3.4 ± 0.8
Naringenin	--	--	--	--	2.8 ± 1.2
Apigenin	--	--	--	--	--
Kaempferol	25.2 ± 2.7	11.6 ± 2.9	7.9 ± 2.2	10.6 ± 1.6	0.9 ± 0.4
Quercetin	70.0 ± 2.4	23.4 ± 2.6	--	--	8.2 ± 3.3
EGCG	105 ± 3.6	45.8 ± 8.2	26.2 ± 5.4	--	--
<b>Prototypic UGT Inhibitors</b>					
Diclofenac	160 ± 11.3	334 ± 74.4	--	--	--
Nicardipine	160 ± 10.0	--	--	--	1.5 ± .4

Apparent IC<sub>50</sub>s were determined by fitting eq. 1, 2, or 3 to observed 4-MU depletion velocities versus nominal inhibitor concentration. Values represent the IC<sub>50</sub> estimate ± S.E. (μM) via nonlinear least-squares regression using Phoenix<sup>®</sup> WinNonlin<sup>®</sup> (version 6.3). --, not determined. UGT1A1, UGT1A8, and UGT1A10 refer to HEK293 cell lysates overexpressing respective individual isoforms.

**Table 2.** Enzyme kinetic parameters for glucuronidation of silybin A and silybin B.

	Enzyme Source					
	HIMs			HLMs		
	$K_m$ or $S_{50}$ ( $\mu\text{M}$ )	$V_{\text{max}}$ (nmol/min/mg)	$Cl_{\text{int}}$ or $Cl_{\text{max}}$ (mL/min/mg)	$K_m$ ( $\mu\text{M}$ )	$V_{\text{max}}$ (nmol/min/mg)	$Cl_{\text{int}}$ (mL/min/mg)
Silybin A	$55 \pm 9.3^a$	$7.6 \pm 1.3^a$	$0.071^a$	$33 \pm 5.2$	$20 \pm 1.1$	0.62
Monoglucuronide 1	$4.2 \pm 0.4$	--	--	$2.0 \pm 0.4$	--	--
Monoglucuronide 2	$27 \pm 2.9$	--	--	$19 \pm 2.9$	--	--
Silybin B	$39 \pm 14$	$94 \pm 14$	2.4	$81 \pm 9.4$	$140 \pm 8.5$	1.7
Monoglucuronide 1	$6.7 \pm 1.0$	--	--	$3.5 \pm 0.5$	--	--
Monoglucuronide 2	$9.8 \pm 1.6$	--	--	$7.6 \pm 1.5$	--	--

Enzyme kinetic parameters ( $K_m$  or  $S_{50}$ ,  $V_{\text{max}}$ ) for glucuronidation of silybin A<sup>a</sup> and silybin B were determined by fitting eq. 4 ( $K_m$ ,  $V_{\text{max}}$ ) or 5 ( $S_{50}$ ,  $V_{\text{max}}$ ) to [substrate] versus substrate depletion (silybin A and silybin B) or metabolite formation (monoglucuronide) velocity data using Phoenix<sup>®</sup> WinNonlin<sup>®</sup>. Values represent the parameter estimate  $\pm$  S.E. Intrinsic clearance ( $Cl_{\text{int}}$ ) was calculated as the ratio of  $V_{\text{max}}$  to  $K_m$ ;  $Cl_{\text{max}}$  was calculated using eq. 6. --, not determined. <sup>a</sup>described best by the Hill equation (eq. 5).

# Figure 1

DMD Fast Forward. Published on July 9, 2014 as DOI: 10.1124/dmd.114.059451  
 This article has not been copyedited and formatted. The final version may differ from this version.

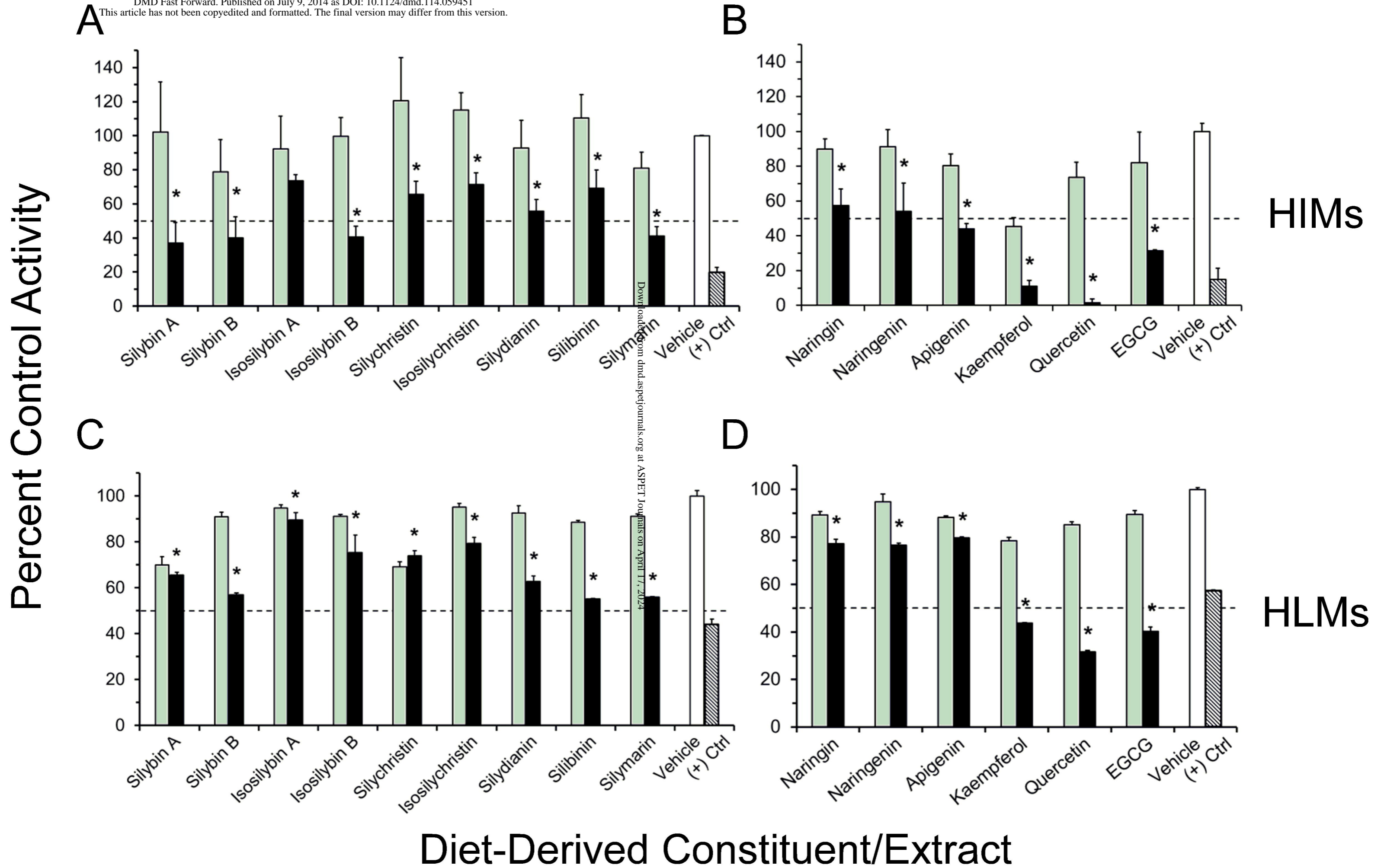
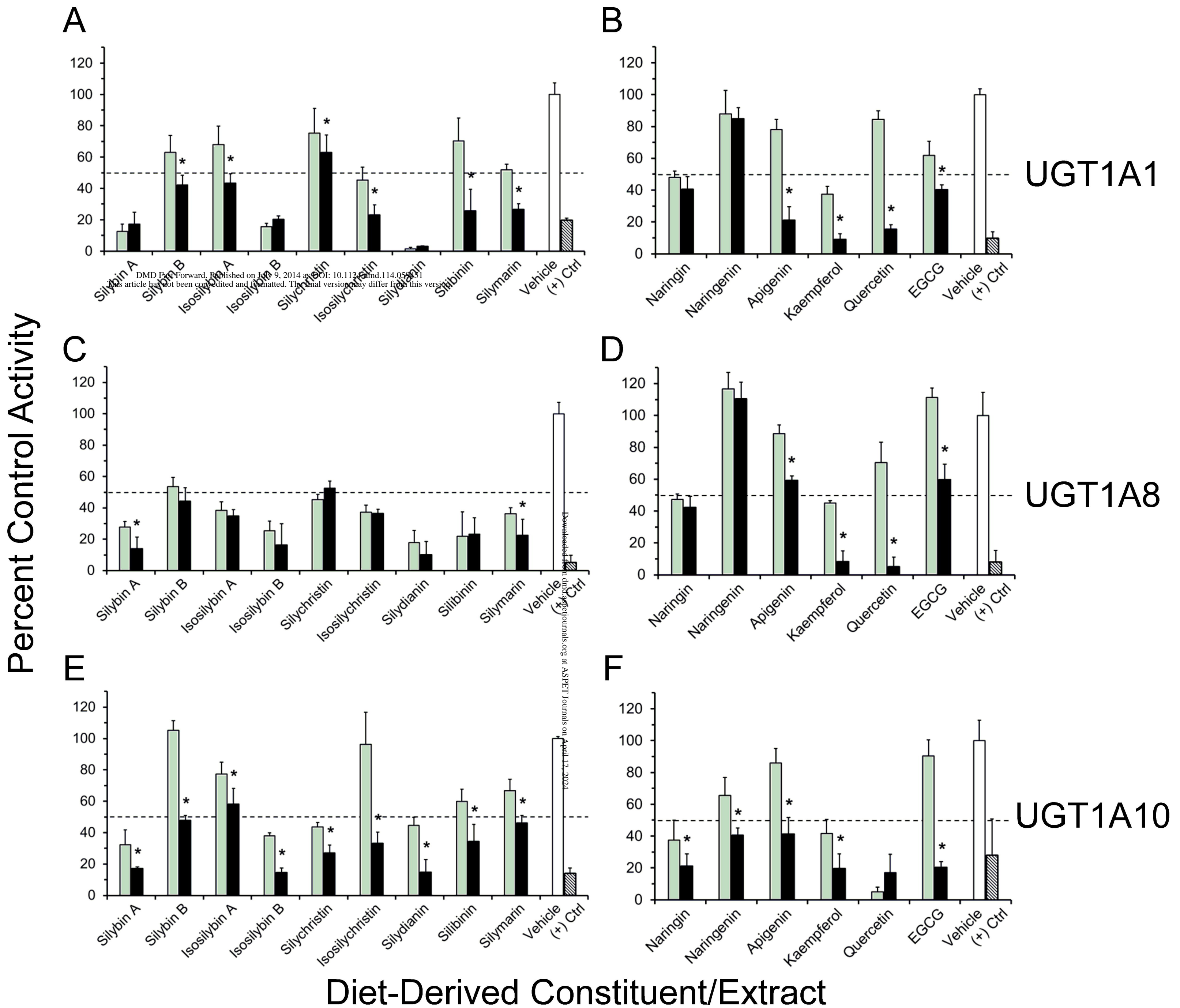


Figure 2





# Figure 3

DMD Fast Forward. Published on July 9, 2014 as DOI: 10.1124/dmd.114.059451  
This article has not been copyedited and formatted. The final version may differ from this version.

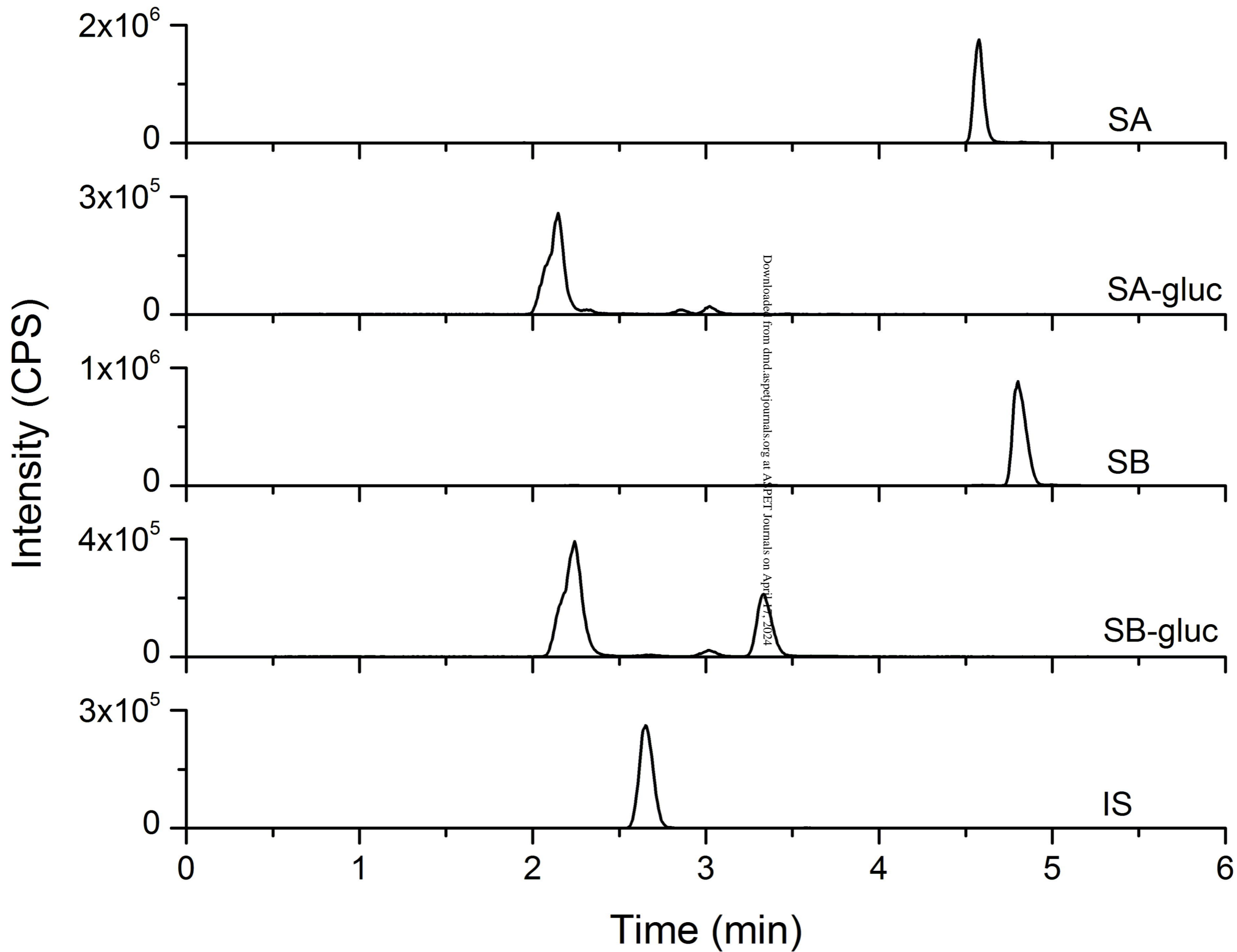


Figure 4

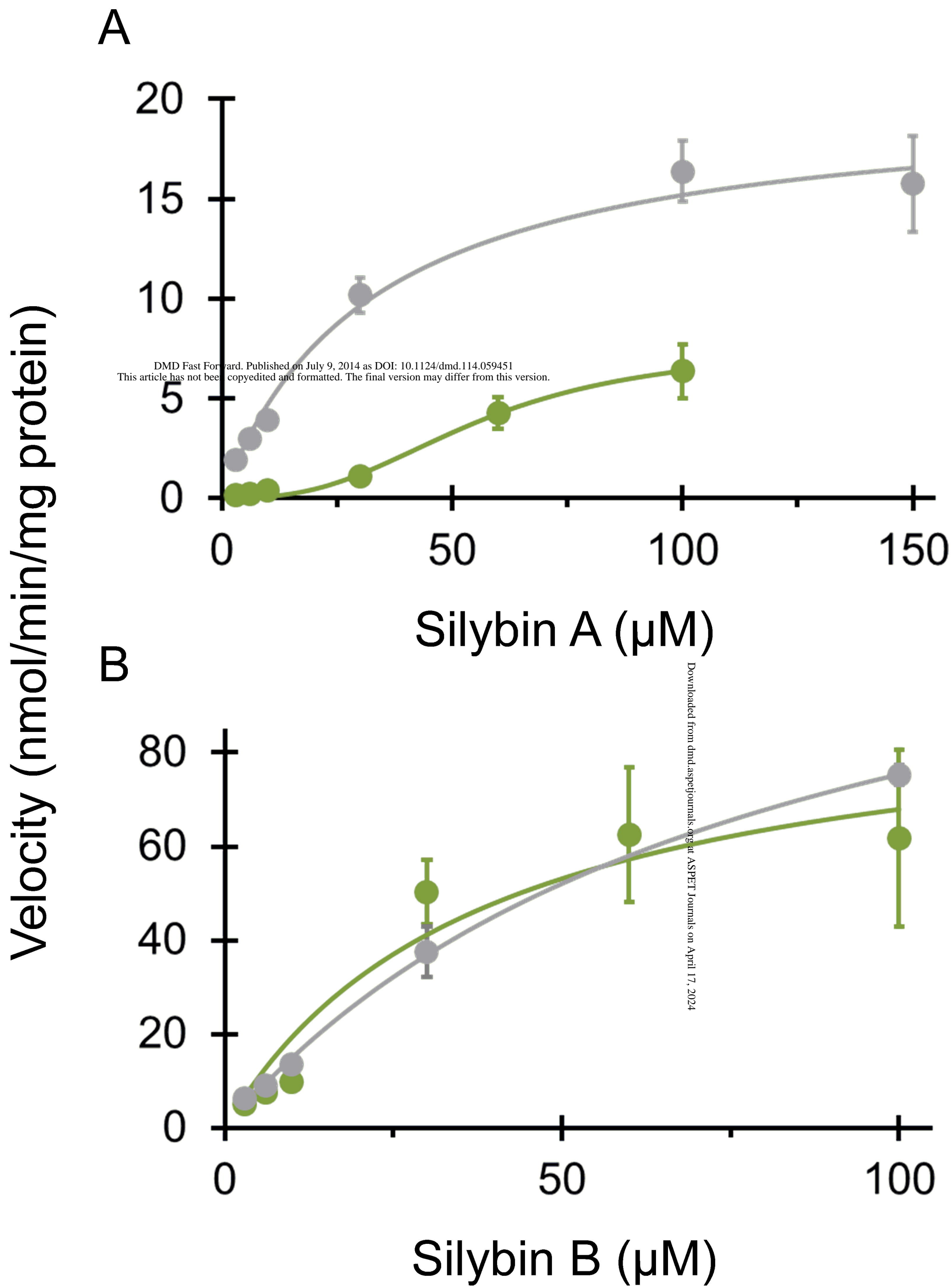
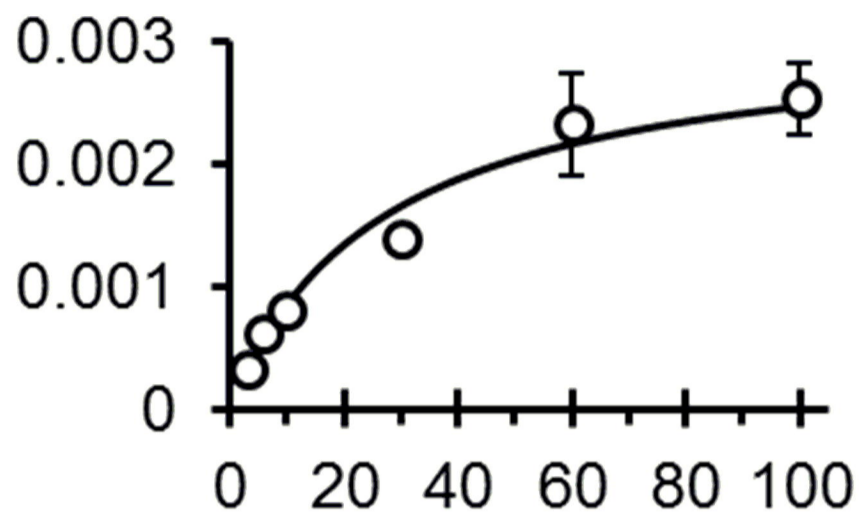
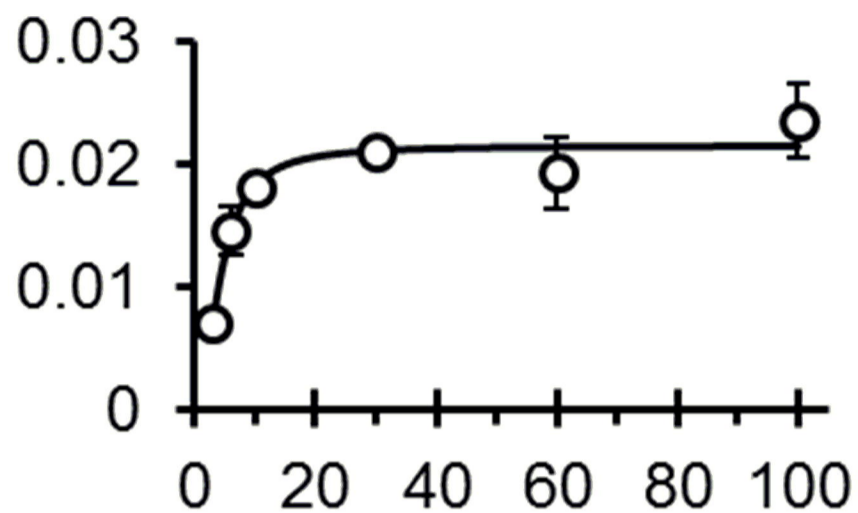


Figure 5

Monoglucuronide 1

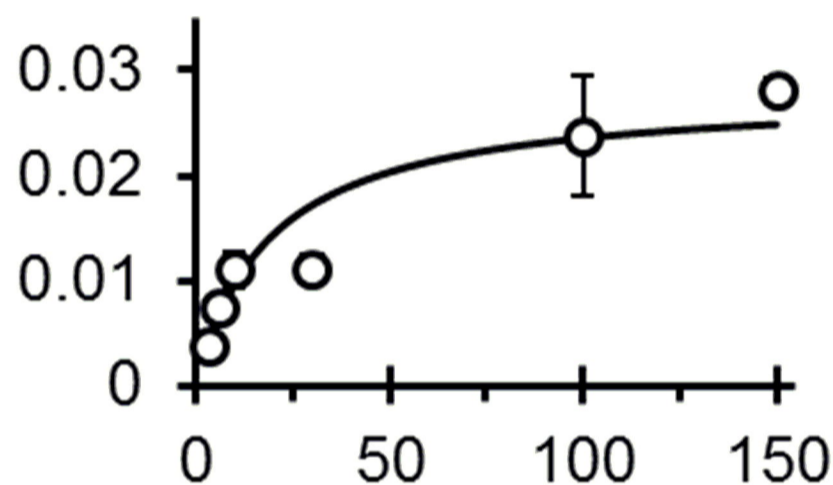
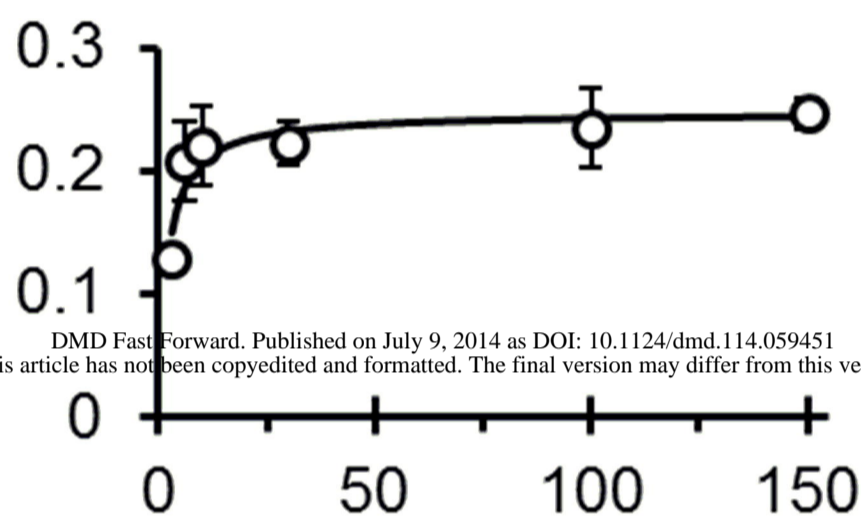
Monoglucuronide 2

A



HIMs

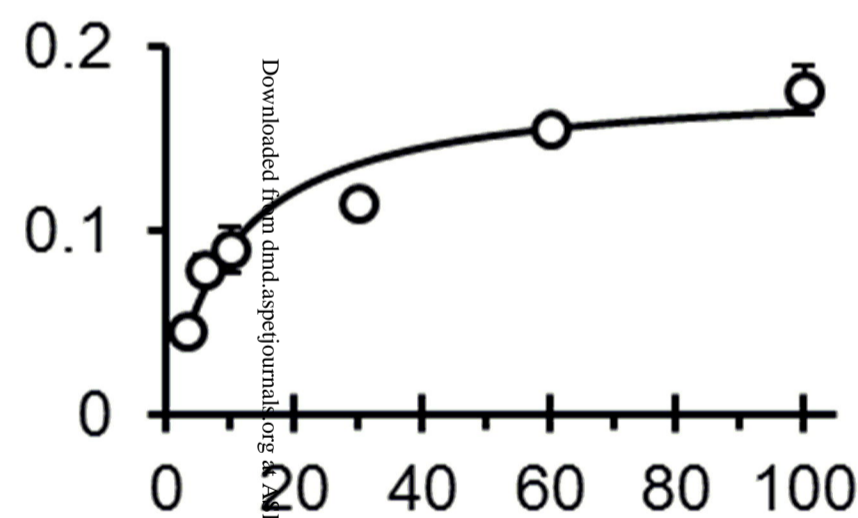
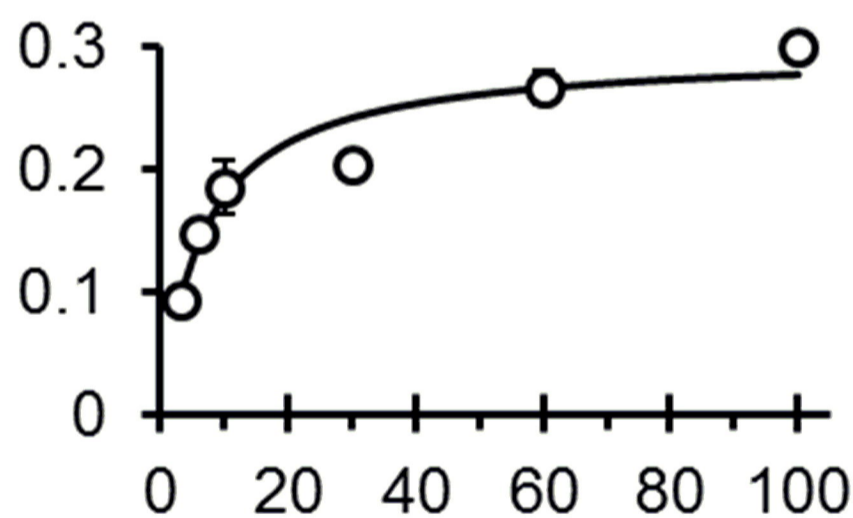
B



HLMs

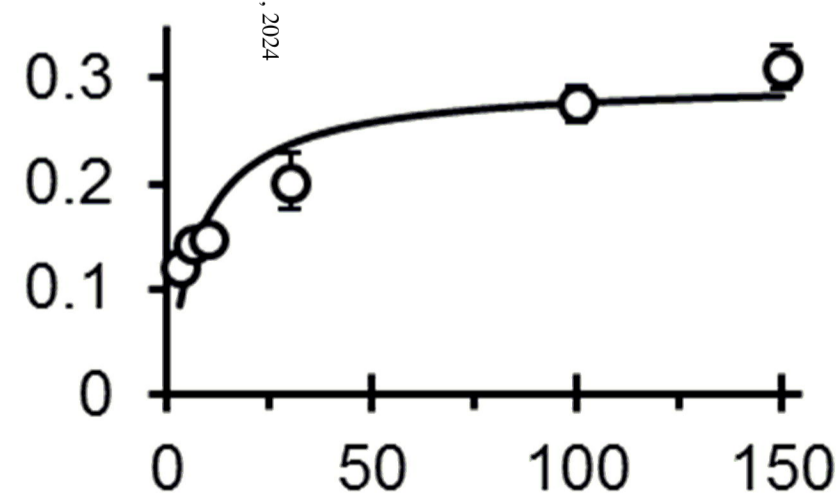
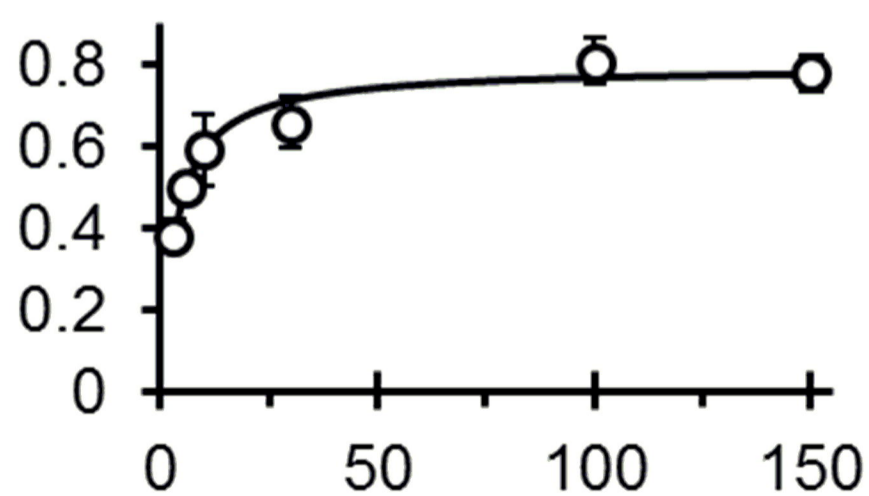
Silybin A (μM)

C



HIMs

D



HLMs

Silybin B (μM)

DMD Fast Forward. Published on July 9, 2014 as DOI: 10.1124/dmd.114.059451  
This article has not been copyedited and formatted. The final version may differ from this version.

Downloaded from dmd.asphjournal.org at MPEI Journals on April 17, 2024

PAR/min

Figure 6

